

IMECE2009-12778

FUZZY SLIDING MODE CONTROL OF A FLEXIBLE SPACECRAFT WITH INPUT SATURATION

Shengjian Bai

College of Mechatronics Engineering and Automation,
National University of Defense Technology
Changsha, Hunan, P. R. China

Qingkun Zhou

College of Mechatronics Engineering and Automation,
National University of Defense Technology
Changsha, Hunan, P. R. China

Pinhas Ben-Tzvi

Department of Mechanical and Aerospace Engineering,
The George Washington University
Washington, DC 20052, USA

Xinsheng Huang

College of Mechatronics Engineering and Automation,
National University of Defense Technology
Changsha, Hunan, P. R. China

ABSTRACT

This paper presents the dynamic modeling and fuzzy sliding mode control (FSMC) for a spacecraft with flexible appendages. A first-order approximate model (FOAM) of the flexible spacecraft system is formulated by using Hamilton's principles and assumed mode method (AMM), taking into account the second-order term of the coupling deformation field. The use of classical Sliding Mode Control (SMC) presents a major problem that appears in the form of chattering. For highly flexible structural models, ideal sliding surface producing pure rigid body motion may not be achievable. In this paper, the discontinuity in the sliding mode controller is smoothed inside a thin boundary layer by using fuzzy logic (FL) techniques so that the chattering phenomenon is effectively reduced. The robustness of SMC only holds in the sliding mode domain (SMD). However, when the amplitude of the actuators is limited, SMD will be restricted to some local domain near zero on the switching surface. Control input saturation is also explicitly considered in the FSMC approach. The new features and advantages of the proposed approach are the use of new dynamic equations of motion of flexible spacecraft systems, and the design of FSMC by taking into account the control input saturation. To study the effectiveness of the corresponding control scheme, the classical

SMC case is also developed for the control system. Numerical simulations are performed to show that rotational maneuvers and vibration suppression are accomplished in spite of the presence of disturbance torques, model uncertainty and control saturation nonlinearity.

KEYWORDS

Dynamic stiffening, Sliding mode control, Fuzzy logic, Flexible spacecraft, Vibrations, Saturation

1. INTRODUCTION

Mechanical systems undergoing high-speed motions can produce dynamic stiffening due to the coupling between rigid motion and elastic deflection [1]. These are hard to be dealt with traditional dynamic analysis techniques. Recent researches indicate that [2, 3] the second order term in the coupling deformation field has a 'stiffening' effect on the frequencies and that the dynamic stiffening is accounted for. In this paper, we take into account the second-order term of the coupling deformation field, and obtain the first-order approximate model (FOAM) of the flexible spacecraft.

Recently, several studies on the control of flexible satellites have been done, and linear and nonlinear control systems have

been designed [4]. But research on the FOAM of flexible spacecrafts is rare [5]. Sliding mode control (SMC) has been known theoretically as a powerful control technique capable of providing very robust control, even invariant under certain condition, with respect to system parameter variations and external disturbances [6]. This superb system performance only holds in the sliding mode domain (SMD) on the whole switching surfaces, which is easily satisfied with ideal control input. However, in practice, the amplitude of the actuators on the spacecraft is limited by physical constraints. Therefore, SMD does not cover the entire switching surface and will be restricted to some local domain near zero on the switching surface. Thus, design of SMC input that is constrained by saturation is studied in this paper. Also, by using fuzzy logic (FL) techniques, the discontinuity in the sliding mode controller is smoothed inside a time-varying boundary layer so that the chattering phenomenon is efficiently reduced.

2. EQUATIONS OF MOTION AND KINEMATICS

As shown in Fig.1, a rigid hub with two elastic beams attached is considered as the model of slewing flexible spacecrafts. The beams represent spacecraft structural elements such as on-board antenna and solar array. Although the design approaches of the present work can be applied to multi-axis maneuvers, for simplicity only single-axis maneuver is considered. The spacecraft is controlled by a torquer on the rigid hub. When the spacecraft is maneuvered, the elastic members connected to the hub experience structural deformation.

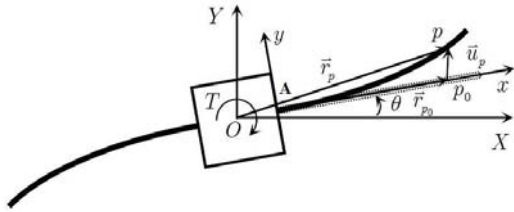


Fig.1: Flexible spacecraft model

The deformation vector u_p can be represented as [2]

$$u_p = (u_1 \quad u_2)^T = (w_1 + w_c \quad w_2)^T \quad (1)$$

where w_1 represents the pure axial deformation of the centroidal axis and w_2 represents the transverse deformation along the y-axis of the reference frame xy . The second order term w_c is

$$w_c = -\frac{1}{2} \int_0^x \left(\frac{\partial w_2}{\partial x} \right)^2 dx \quad (2)$$

It should be noted that this term can have a significant impact on the beam's dynamic equations when it undergoes large rigid-body motion.

By using assumed mode method (AMM) and Lagrangian principle, the FOAM of the flexible spacecraft can be derived as [3]:

$$\begin{bmatrix} M_{\theta\theta} & M_{\theta q_1} & M_{\theta q_2} \\ M_{q_1\theta} & M_{q_1 q_1} & \mathbf{0} \\ M_{q_2\theta} & \mathbf{0} & M_{q_2 q_2} \end{bmatrix} \begin{bmatrix} \ddot{\theta} \\ \ddot{q}_1 \\ \ddot{q}_2 \end{bmatrix} + 2\dot{\theta} \begin{bmatrix} 0 & \mathbf{0} & \mathbf{0} \\ 0 & \mathbf{0} & G_{q_1 q_2} \\ 0 & G_{q_2 q_1} & \mathbf{0} \end{bmatrix} \begin{bmatrix} \dot{\theta} \\ \dot{q}_1 \\ \dot{q}_2 \end{bmatrix} + \begin{bmatrix} 0 & \mathbf{0} & \mathbf{0} \\ 0 & K_{q_1 q_1} & \mathbf{0} \\ 0 & \mathbf{0} & K_{q_2 q_2} \end{bmatrix} \begin{bmatrix} \theta \\ q_1 \\ q_2 \end{bmatrix} = \begin{bmatrix} Q_\theta \\ Q_{q_1} \\ Q_{q_2} \end{bmatrix} + \begin{bmatrix} \tau \\ \mathbf{0} \\ \mathbf{0} \end{bmatrix} \quad (3)$$

where $M_{\theta\theta} \in R^1$ is the rotary inertia of the system, $M_{q_1 q_1} \in R^{n \times n}$ and $M_{q_2 q_2} \in R^{n \times n}$ are the beam generalized elastic mass matrices, $M_{\theta q_1} \in R^{1 \times n}$, $M_{\theta q_2} \in R^{1 \times n}$, $M_{q_1 \theta} \in R^{n \times 1}$ and $M_{q_2 \theta} \in R^{n \times 1}$ represent the nonlinear inertia coupling between the motion of the reference frame and the elastic deformations, $K_{q_1 q_1} \in R^{n \times n}$ and $K_{q_2 q_2} \in R^{n \times n}$ are generalized elastic stiffness matrices that are shown to be affected by both the motion of the reference frame and the elastic deformations, Q_θ represents inertia forces, τ is the rotational external torque. The parameters in Eq.(3) can be referred to in reference [3].

The newly established Eq.(3) is called FOAM. Eq.(3) without the terms induced by the second order term w_c is called traditional linear approximate model (TLAM), which is widely used to investigate the dynamics and control of flexible spacecrafts. A simplified first-order approximate model (SFOAM) of the flexible spacecraft can be derived from FOAM by deleting the elements related to Q_θ , q_1 and \dot{q}_1 :

$$\begin{bmatrix} M_{\theta\theta} & M_{\theta q_2} \\ M_{q_2\theta} & M_{q_2 q_2} \end{bmatrix} \begin{bmatrix} \ddot{\theta} \\ \ddot{q}_2 \end{bmatrix} + \begin{bmatrix} 0 & \mathbf{0} \\ \mathbf{0} & K_{q_2 q_2} \end{bmatrix} \begin{bmatrix} \theta \\ q_2 \end{bmatrix} = \begin{bmatrix} \tau \\ \mathbf{0} \end{bmatrix} \quad (4)$$

where $M_{\theta\theta}$, $M_{\theta q_2}$, $M_{q_2 \theta}$, $M_{q_2 q_2}$ and $K_{q_2 q_2}$ can also be obtained by deleting the elements related to q_1 and \dot{q}_1 in Eq.(3).

It is noted that SFOAM will be used for controller design.

3. FUZZY SLIDING MODE CONTROLLER DESIGN WITH INPUT SATURATION

In order to maneuver the rotation angle from θ_0 to θ_d , we design control law $u(t)$ which satisfies

$$\begin{aligned} \lim_{t \rightarrow \infty} q_i(t) &= \lim_{t \rightarrow \infty} \dot{q}_i(t) = 0 & (i = 1, 2, \dots, n) \\ \lim_{t \rightarrow \infty} \theta(t) &= \theta_d, \quad \lim_{t \rightarrow \infty} \dot{\theta}(t) = 0 \end{aligned} \quad (5)$$

3.1 Design of sliding mode control

Next, the reaching law method and fuzzy time-varying boundary layer thickness are adopted to achieve a trade-off between tracking precision and robustness to modeling inaccuracies.

Consider the following nonlinear system:

$$\text{Plant: } \quad x^{(n)}(t) = f(\mathbf{x}, t) + b(\mathbf{x}, t)u(t) + d(t) \quad (6)$$

$$\text{Model: } \quad x^{(n)}(t) = \hat{f}(\mathbf{x}, t) + \hat{b}(\mathbf{x}, t)u(t) \quad (7)$$

where $\mathbf{x} = [x, \dot{x}, \dots, x^{(n-1)}]^T$ is the state vector, $u(t)$ is the scalar control input, and $d(t)$ is the external disturbance. Assume the nonlinear function $f(\mathbf{x}, t)$ and $d(t)$ are not exactly known, however

$$f(\mathbf{x}, t) = \hat{f}(\mathbf{x}, t) + \Delta f(\mathbf{x}, t) \quad (8)$$

$$|\Delta f(\mathbf{x}, t)| < F(\mathbf{x}, t) \quad (9)$$

$$|d(t)| < D(t) \quad (10)$$

where $\hat{f}(\mathbf{x}, t)$, $\Delta f(\mathbf{x}, t)$ and $F(\mathbf{x}, t)$ represent the known model of the system, model uncertainties, and upper bound for uncertainties, respectively; and $D(t)$ is the upper bound of $d(t)$. Furthermore, assume that $b(\mathbf{x}, t)$ is not exactly known, however

$$0 < b_{\min} < b(\mathbf{x}, t) < b_{\max}, b(\mathbf{x}, t) \neq 0 \quad \forall t \quad (11)$$

and

$$\hat{b}(\mathbf{x}, t) = (b_{\min} b_{\max})^{1/2} \quad (12)$$

Let $\mathbf{e} = \mathbf{x} - \mathbf{x}_d = [x - x_d, \dot{x} - \dot{x}_d, \dots, x^{(n-1)} - x_d^{(n-1)}]$ be the tracking error. Furthermore, let us define a time-varying sliding surface $s(\mathbf{e})$ with

$$s(\mathbf{e}) = \sum_{i=1}^n c_i e_i \quad c_n = 1 \quad \text{and} \quad c_i > 0 \quad (13)$$

where $e_i = x^{(i-1)} - x_d^{(i-1)}$, for $i = 1, 2, \dots, n$, and the characteristic polynomial of Eq. (13) is Hurwitz. The design parameters c_i determine the speed of response in sliding mode and steady state response of the system, which will be discussed in the next section.

Three approaches for specifying the reaching condition have been presented in [6].

a) The direct switching function approach

$$s\dot{s} < 0 \quad (14)$$

b) The Lyapunov function approach

$$s\dot{s} < -\eta|s| \quad (15)$$

where η is a positive constant.

c) The reaching law approach

$$\dot{s} = -\eta \text{sgn}(s) - ks \quad (16)$$

where η and k are positive constants. The reaching condition (14) is global but does not guarantee a finite reaching time. On the other hand, the reaching law (15) and (16) not only have global characteristics, but also guarantee a finite reaching time.

A thin boundary layer neighboring the switching surface is used here to smooth out the control discontinuity.

$$B(\mathbf{x}, t) = \{x, |s(\mathbf{x}, t)| \leq \phi(t)\} \quad \phi(t) > 0 \quad (17)$$

where $\phi(t)$ is the boundary layer thickness.

The control input $u(t)$ in (6) is made to satisfy the following reaching condition [6]:

$$s\dot{s} \leq -(\eta - \dot{\phi})|s| \quad (18)$$

where η is a strictly positive constant.

Differentiating (13) and rearranging it using (6) we obtain

$$\dot{s} = \sum_{i=1}^{n-1} c_i e_{i+1} - x_d^{(n)} + f(\mathbf{x}, t) + b(\mathbf{x}, t)u(t) + d(t) \quad (19)$$

Combining the reaching condition (18) and the reaching law (16), we obtain a novel reaching law with time-varying boundary layer:

$$\dot{s} = -(\eta - \dot{\phi}) \text{sat}(s/\phi) - ks \quad (20)$$

where

$$\text{sat}(s/\phi) = \begin{cases} s/\phi, & \text{for } |s/\phi| \leq 1 \\ \text{sgn}(s/\phi), & \text{for } |s/\phi| > 1 \end{cases} \quad (21)$$

The merits of the proposed novel reaching law (20) are: (i) chattering can be reduced by tuning parameters η and k [7]; and (ii) the boundary layer is used here to achieve a trade-off between tracking precision and robustness.

Then we can derive the control input from (6), (7) and (20) as follows:

$$u(t) = \hat{u}(t) - \hat{b}^{-1}(\mathbf{x}, t)k(\mathbf{x}, t)\text{sat}(s/\phi) \quad (22)$$

$$\hat{u}(t) = \hat{b}^{-1}(\mathbf{x}, t) \left[x_d^{(n)} - \sum_{i=1}^{n-1} c_i e_{i+1} - \hat{f}(\mathbf{x}, t) - k \sum_{i=1}^n c_i e_i \right] \quad (23)$$

where

$$k(\mathbf{x}, t) = b^{-1}(\mathbf{x}, t) \hat{b}(\mathbf{x}, t) \left[F(\mathbf{x}, t) + D(t) + \eta - \dot{\phi}(t) \right] + \left| b^{-1}(\mathbf{x}, t) \hat{b}(\mathbf{x}, t) - 1 \right| \left| \hat{u}(t) \right| \quad (24)$$

Note that

$$b^{-1}(\mathbf{x}, t) \hat{b}(\mathbf{x}, t) \leq \beta$$

where $\beta = (b_{\max}/b_{\min})^{1/2}$.

Rewrite Eq.(24), we derive:

$$k(\mathbf{x}, t) = \beta \left[F(\mathbf{x}, t) + D(t) + \eta - \dot{\phi}(t) \right] + (\beta + 1) \left| \hat{u}(t) \right| \quad (25)$$

We can see that, the control parameter $k(\mathbf{x}, t)$ has been increased in order to account for the uncertainty on the control gain b , parameter uncertainty and disturbance.

3.2 Design of fuzzy boundary layer

Chattering in the control signal is one of the most important problems met in sliding mode control applications. Different methods have been presented in the literature [8, 9]. Utkin [8] investigated the chattering problem in sliding mode control systems, and pointed out that, the chattering amplitude can be reduced for discontinuous control with state dependent gain. In fact, the boundary layer approach adopts the similar idea. It is indicated that [9], the determination of a suitable boundary layer thickness which will assure best performance and still eliminate chattering. Next, we will use FL to on-line tune the boundary layer thickness. The fuzzy boundary layer leads to a strategy that adjusts the thickness of the boundary ϕ automatically. This fuzzy system adopts the sliding surfaces s and its derivation \dot{s} as inputs and the thickness ϕ of the boundary layer as the output.

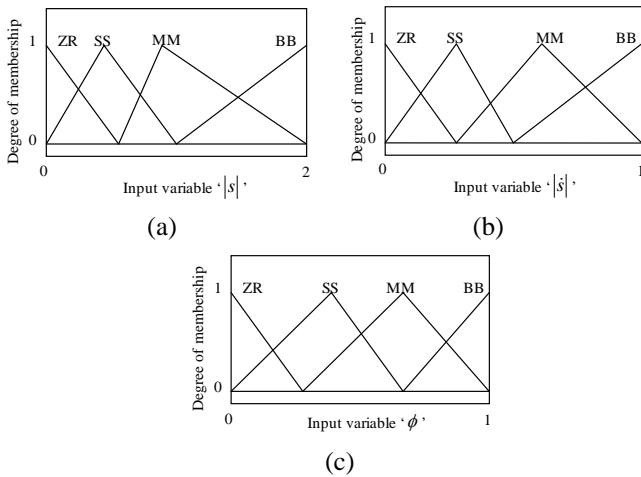


Fig.2: Membership functions

The multiple input single output rule base is presented in Tab.1, where ZR, SS, MM and BB stand for zero, positive small,

positive medium and positive big. An example fuzzy rule in Tab.1 is:

IF $|s|$ is BB AND $|\dot{s}|$ is BB THEN ϕ is BB

where “AND” is defined by μ_A AND $\mu_B = \mu_A \times \mu_B$ for any two membership values μ_A and μ_B over the fuzzy subsets A and B, respectively.

This can be implied that IF the state trajectory is far from the sliding surface AND moves fast, THEN the thickness of the boundary layer should be big. The results derived by using those fuzzy rules are shown in Fig.3. The results show that the thickness of the boundary layer can be well tuned, according to the distance of the state point to sliding surface and its derivation. Relevant discussions can refer to [9].

Tab.1: The fuzzy rules for $|s|$, $|\dot{s}|$ and ϕ

ϕ	$ s $				
	ZR	SS	MM	BB	
$ \dot{s} $	ZR	ZR	ZR	SS	SS
	SS	ZR	SS	SS	MM
	MM	SS	SS	MM	BB
	BB	SS	MM	BB	BB

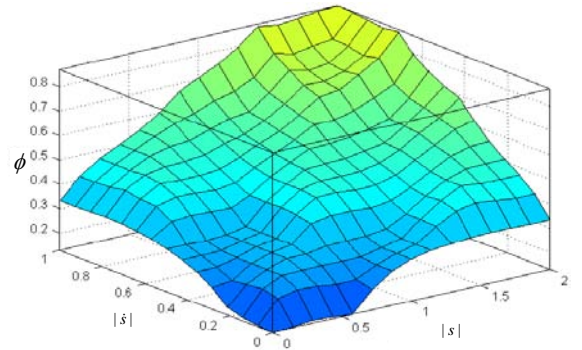


Fig.3: The 3D plot of $|s|$, $|\dot{s}|$ and ϕ

3.3 Design of linear switching line with bounded inputs

In this section, we will investigate the sliding mode domain (SMD) of SMC with bounds on the control action. The aim is to achieve robustness in the maximized sliding mode domain on the switching surfaces.

Firstly, we consider the design of SMC for a single-input LTI system with bounded input:

$$\dot{x} = \mathbf{A}x + \mathbf{B}u \quad |u| \leq K, \quad K > 0 \quad (26)$$

The state vector x is n -dimensional. \mathbf{A} and \mathbf{B} are constant matrices of appropriate dimensions. A linear switching surface is selected

$$s := \mathbf{S}x = 0 \quad (27)$$

where \mathbf{S} is n -dimensional vector, $\mathbf{S}\mathbf{B}=1$, and $(n-1)$ poles of the equivalent system are stable

$$\dot{x} = (\mathbf{I} - \mathbf{B}\mathbf{S})x \quad (28)$$

where \mathbf{I} is a unit matrix.

The bounded control law

$$u = -K \text{sgn}(s) \quad (29)$$

is considered. Then the question asked is how to select the switching surface $s(x)=0$ to maximize the SMD.

The closed loop system can be viewed as Lur'e-type system, i.e., the memoryless nonlinear feedback part (29) to the forward LTI system belongs to the sector $[0, \infty)$. If the transfer function of the linear subsystem is so-called positive real, then it has important properties which may lead to the generation of a Lyapunov function for the whole system.

The following theorem is valid.

Theorem 1 For the system (1), if A is Hurwitz and (\mathbf{A}, \mathbf{B}) is controllable, then by choosing the stable switching surface

$$s(x) := \mathbf{S}x = 0 \quad (30)$$

where $\mathbf{S}\mathbf{B}=1$ and (\mathbf{S}, \mathbf{A}) is observable.

Then SMD is

$$D := \{x | \mathbf{S}x = 0, -K < \mathbf{S}\mathbf{A}x < K\} \quad (31)$$

and the initial state from any point of the state space approaches to the SMD within finite time. \square

Proof Firstly, considering the linear switching surface (30), and reaching condition[6], we have

$$\begin{cases} \dot{s} = \mathbf{S}(\mathbf{A}x + \mathbf{B}K) > 0 & s < 0 \\ \dot{s} = \mathbf{S}(\mathbf{A}x - \mathbf{B}K) < 0 & s > 0 \end{cases} \quad (32)$$

That is $-K < \mathbf{S}\mathbf{A}x < K$, so the SMD is given by (31).

Secondly, considering that the LTI system is a minimum realization of the strict positive transfer function, then the LTI system is strictly passive [7]. A radial unbounded Lyapunov function can be chosen as a storage function by using KYP lemma as in [7]. This guarantees that the closed loop system is globally exponentially stable. So if a ball N near zero is considered such that

$$N(x, \gamma) := \{x \in R^n | \|x\| \leq \gamma\} \quad (33)$$

where

$$0 < \gamma \leq \frac{K}{\|\mathbf{S}\mathbf{A}\|} \quad (34)$$

then the initial state from any point of the state space reaches inside the ball within finite time. That is, the initial state from any point of the state space approaches to the SMD described in (31) within finite time. \square

The control law (29) guarantees that the trajectory of the solution starting from any initial state of (26) reaches to the SMD (31) on the switching surface within a finite time and approaches to zero thereafter.

Next, a rigid spacecraft undergoing single-axis maneuver will be investigated for simplicity

$$J\ddot{\theta} = T \quad (35)$$

where J is the rotational inertia of the rigid spacecraft, T is the constant rotational torque, which is constrained by

$$|T| \leq K, \quad K > 0 \quad (36)$$

Without loss of generality, it is assumed that the flexible spacecraft maneuvers from an initial angle θ_0 to $\theta_d = 0$. A linear switching line is defined as

$$s = \dot{\theta} + c\theta, \quad c > 0 \quad (37)$$

where c is the slope of the linear switching line, which cannot be chosen arbitrarily with bounded inputs.

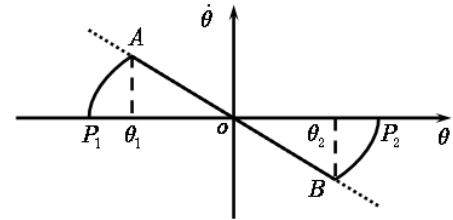


Fig.4: Sliding mode domain on linear switching line

As shown in Fig.4, P_1 and P_2 are the initial points $(\theta_0, 0)$ in the phase plane. With the restriction of the control input (36), it can be derived from the **theorem 1** that the SMD on the switching line is restrained to the local domain AB near zero:

$$D_{SMD} = \left\{ (\theta, \dot{\theta}) \mid \dot{\theta} + c\theta = 0, |\theta| < \frac{\sqrt{K^2 - 2KJc^2\theta_0} - K}{Jc^2} \right\} \quad (38)$$

The SMD is maximized when the optimized coefficient c is chosen as

$$c^* = \sqrt{\frac{3K}{2J|\theta_0|}} \quad (39)$$

4. SIMULATIONS AND RESULTS

In this section, simulation results for the dynamics of a flexible spacecraft are presented using Mathematica and Visual C++. A slewing maneuver of the spacecraft is used to

demonstrate the applicability of the FSMC presented in Sections 2 and 3. A 4th-order Runge-Kutta program with adaptive step-size is used to numerically solve the differential equations. The physical parameters of the rigid-flexible system are shown in Tab.2.

Tab.2: Physical parameters

Property	Symbol	Value
Beam length	L	12m
Mass per unit volume	ρ	$2.8 \times 10^3 \text{ kg/m}^3$
Cross-Section	A	$7.5 \times 10^{-5} \text{ m}^2$
Young's modulus	E	$7.0 \times 10^{10} \text{ N/m}^2$
Beam area moment of inertia	I	$7.2 \times 10^{-9} \text{ m}^4$
Hub moment of inertia	J_h	500 kgm^2
Hub radius	r	0.5m

4.1 Free vibrations of the flexible spacecraft system

Consider the flexible spacecraft model, as shown in Fig.1. We will investigate the free vibration of FOAM and TLAM. The angular velocity of the hub starts from zero according to the following profile

$$\dot{\theta} = \begin{cases} \frac{w_0}{T}t - \frac{w_0}{2\pi} \sin\left(\frac{2\pi}{T}t\right) & 0 \leq t \leq T \\ w_0 & t > T \end{cases} \quad (40)$$

where $T = 10s$, $w_0 = 6rad/s$.

Fig. 5 shows the tip deflection of the beam by using the two models. It can be seen that there is a significant difference between the tip deflections by using the TLAM (dashed line) compared to the FOAM (solid line). We can see that, the amplitude of the resulting tip deflection using the TLAM becomes much larger compared to when using the FOAM at $t = 3.5s$. Moreover, the resulting tip deflection using the TLAM has exceeded the small deformation assumption. Because the second order term in deformation field is not included, the elastic stiffness matrix may be negative definite and the system becomes unstable. From the above, it is shown that the second order term in the deformation field can have significant effect on the dynamic behavior of flexible multibody systems.

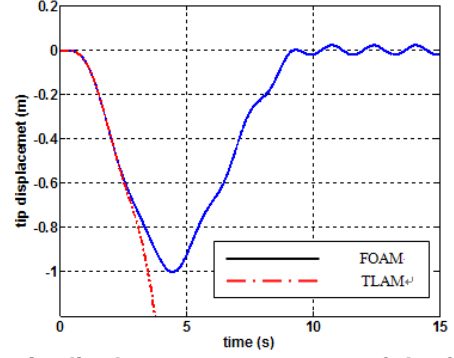


Fig.5: The tip displacement response of the flexible appendages

4.2 Fuzzy sliding mode control of the flexible spacecraft

By rearranging Eq.(4), we can derive

$$\left(M_{\theta\theta} - M_{\theta q_2} M_{q_2 q_2}^{-1} M_{q_2 \theta}\right) \ddot{\theta} = \tau + M_{\theta q_2} M_{q_2 q_2}^{-1} K_{q_2 q_2} q_2 \quad (41)$$

The control input can be obtained the same way as in Eq.(22)

$$\tau = \hat{u}(t) - \hat{b}^{-1}(x, t) k(x, t) \text{sat}(s/\phi) \quad (42)$$

where

$$\hat{u}(t) = -\left(M_{\theta\theta} - M_{\theta q_2} M_{q_2 q_2}^{-1} M_{q_2 \theta}\right) c \dot{\theta} - M_{\theta q_2} M_{q_2 q_2}^{-1} K_{q_2 q_2} q_2 \quad (43)$$

$$k(x, t) = \beta \left[\alpha |f(x, t)| + D(t) + \eta - \dot{\phi}(t) \right] + (\beta + 1) |\hat{u}(t)| \quad (44)$$

where

$$f(x, t) = \frac{M_{\theta q_2} M_{q_2 q_2}^{-1} K_{q_2 q_2} q_2}{M_{\theta\theta} - M_{\theta q_2} M_{q_2 q_2}^{-1} M_{q_2 \theta}} \quad (45)$$

The proposed controller derived from SFOAM is used for rest-rest attitude maneuvering of the FOAM. Our aim is to maneuver the attitude of the spacecraft from $\theta_0 = 2rad$ to $\theta_d = 0$, and suppress the flexible vibrations simultaneity. The control parameters are selected to be $\hat{b} = 1$, $\beta = 2$, $\alpha = 0.2$, $D(t) = 0$, $\eta = 0$, $c^* = 0.2$, and $K = 50Nm$.

Although we are dealing with infinite-dimensional system, it is impossible to use infinite number of modes in the simulation. To make the simulation more meaningful, two measures are taken: (i) a relative large number of flexible modes is chosen in the FOAM, which are used for the simulation; (ii) feedback signals associated with flexibility are assumed to be from the first mode, because the lower frequency component is dominant [8]. Thus, the assumed mode n of the FOAM and SFOAM is chosen as 5 and 1, respectively.

Fig. 6 shows the attitude angle of the flexible spacecraft. It can be seen that, attitude angle control was accomplished in the closed-loop system. When c is chosen as 0.5, the time

response of the attitude angle has overshoot. When c is chosen as 0.1, long settling time will be endured. In the control of the flexible appendage, what we are concerned with is the motion of the tip. Accordingly, the tip motion of the appendages is given in Fig.7. We can find that for larger or smaller c values, both exhibit larger tip deformation. Thus, the parameter c discussed in Section 3.3 not only meets precision requirements of the attitude angle, but also results in smaller tip deformation. The bounded control input is shown in Fig.8. It can be seen that the use of boundary layer eliminates the chattering and generates a continuous control.

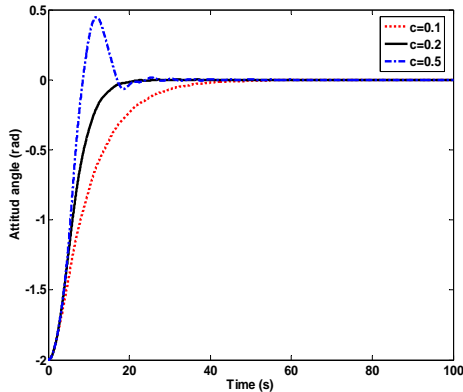


Fig.6: Attitude angle

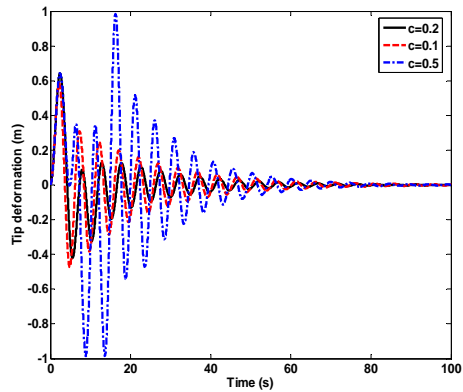


Fig.7: Tip deformation of flexible appendages

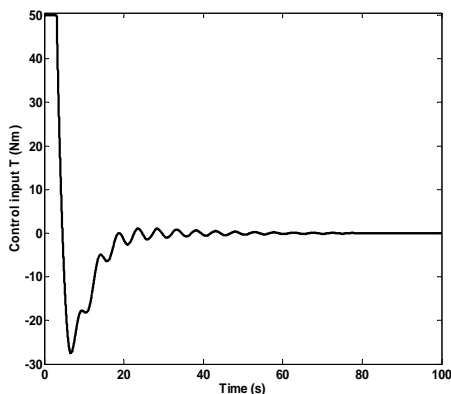


Fig.8: Control input

5. CONCLUSIONS

This paper presented the development of the FOAM and SFOAM methods for a flexible spacecraft. The free vibration of the FOAM and TLAM has been investigated to illustrate the validity of the FOAM when experiencing high rotational speeds. The proposed control law has been presented by utilizing FL and SMC theory with input saturation. Numerical simulations were provided to show the effectiveness of the presented controller in the rotational maneuver and vibration suppression in spite of the presence of model uncertainty and control saturation nonlinearity.

REFERENCES

- [1] Kane, T.R., Ryan, R.R., Banerjee, A.K., 1987, "Dynamics of a cantilever beam attached to a moving base", *Journal of Guidance, Control, and Dynamics*, **10(2)**, pp. 139-150.
- [2] Liu, J., Hong, J., 2004, "Geometric stiffening effect on rigid-flexible coupling dynamics of an elastic beam", *Journal of Sound and Vibration*, **278(4)**, pp. 1147-1162.
- [3] Bai, S., Ben-Tzvi, P., Zhou, Q., Huang, X., 2009, "A study on dynamic stiffening of a rotating beam with a tip mass", *Sensors & Transducers Journal*, **5**, pp. 53-68.
- [4] Hyland, D.C., Junkins, J.L., Longman, R.W., 1993, "Active control technology for large space structures", *Journal of Guidance, Control, and Dynamics*, **16(5)**, pp. 801-821.
- [5] Cai, G., Hong, J., 2005, "Active position control of a flexible manipulator", *Mechanical Science and Technology*, **24(1)**, pp. 70-74.
- [6] Hung, J.Y., Gao, W.B., Hung, J.C., 1993, "Variable structure control. A survey", *IEEE Transactions on Industrial Electronics*, **40(1)**, pp. 2-22.
- [7] Slotine, J.-J.E., Li, W., 2004, *Applied Nonlinear Control*, China Machine Press.
- [8] Utkin, V., Lee, H., June, 2006, "Chattering problem in sliding mode control systems", *Proceedings of the 2006 International Workshop on Variable Structure Systems*, pp. 346-350.
- [9] Erbaturo, K., Kaynak, O., 2001, "Use of Adaptive Fuzzy Systems in Parameter Tuning of Sliding-Mode Controllers", *IEEE/ASME TRANSACTIONS ON MECHATRONICS*, **6(4)**, pp. 474-482.